Free Precession and Transverse Relaxation of Hyperpolarized ^{129}Xe Gas Detected by SQUIDs in Ultra-Low Magnetic Fields

W. Kilian[1a], A. Haller[1b], F. Seifert[1], D. Grosenick[1], and H. Rinneberg[1]

Physikalisch-Technische Bundesanstalt, Abbestraße 2-12, D-10587 Berlin, Germany

Eur. Phys. J. D / Received: 07.08.2006 / Revised version: 22.12.2006 / Accepted: 12.01.2007

Abstract. We studied the free precession of the nuclear magnetization of hyperpolarized ^{129}Xe gas in external magnetic fields as low as $B_0 = 4.5$ nT, using SQUIDs as magnetic flux detectors. The transverse relaxation was mainly caused by the restricted diffusion of ^{129}Xe in the presence of ambient magnetic field gradients. Its pressure dependence was measured in the range from 30 mbar to 850 mbar and compared quantitatively to theory. Motional narrowing was observed at low pressure, yielding transverse relaxation times of up to 8000 s.

PACS. 82.56.Na Relaxation – 82.56.Lz Diffusion – 51.20.+d Viscosity, diffusion, and thermal conductivity – 85.25.Dq Superconducting quantum interference devices (SQUIDs)

1 Introduction

Optical pumping of rare gases (^{3}He, ^{129}Xe) makes it possible to achieve a nuclear polarization of up to several ten percent [1–3]. Such hyperpolarized gases have found many fields of application, e.g. as neutron spin filters and polarized nuclear targets (^{3}He) [3,4], for tests of fundamental symmetries (^{3}He, ^{129}Xe) [5,6], for magnetic resonance imaging (MRI) of the lungs (^{3}He, ^{129}Xe) [7,8] and for ^{129}Xe MR-spectroscopy of the brain [9,10].

In the following, we report on the pressure dependence of the transverse relaxation of hyperpolarized ^{129}Xe in xenon gas of natural abundance. The gas was contained in a spherical glass bulb at room temperature. For the detection of the ^{129}Xe magnetization we applied instrumentation which is commonly used for investigations of biomagnetism, i.e. superconducting quantum interference devices (SQUIDs) inside a magnetically shielded room with residual magnetic fields of only a few nT. The transverse relaxation was mainly caused by gaseous diffusion in the presence of magnetic field gradients. As the gas pressure inside the glass bulb becomes sufficiently low, one reaches the regime of restricted diffusion. We were thus able to test, for the first time, an existing theory [11] of spin relaxation in the motional narrowing regime directly, exploiting thereby the high sensitivity of SQUIDs, the small residual magnetic fields and the small ambient magnetic field gradients inside the magnetically shielded room.

In earlier studies, the magnetic field generated by hyperpolarized ^{3}He gas which was contained in a glass bulb that was located in a magnetically shielded environment was measured at a resolution of 100 fT by Cohen-Tannoudji et al. [12], using a ^{87}Rb magnetometer. More recently, a single-channel low-T_c DC SQUID second-order gradiometer operated in an unshielded environment has been employed to measure the spin precession of hyperpolarized ^{3}He in the earth's magnetic field [13]. Recently, also SQUID-detected NMR of laser-polarized solid ^{129}Xe at 4.2 K [14] and SQUID MRI of laser polarized gaseous ^{3}He and solid ^{129}Xe at 4.2 K [15] have been reported, employing, however, magnetic fields in the μT range which are several (3-6) orders of magnitude larger than the fields used in our study.

2 Materials

We produced hyperpolarized ^{129}Xe ($I = 1/2$) off-line by spin-exchange optical pumping, using circularly polarized laser radiation to exite the D_1 transition of Rb [1]. For optical pumping, a cylindrical Duran glass cell ($V = 30\,\mathrm{cm}^3$, inner diam.: 1.9 cm) was filled with typically 850 mbar of xenon (natural abundance: ^{129}Xe = 26.4%), 200 mbar of N_2 and a drop of Rb metal. The cell was placed in a holding field of $B_0 \approx 10$ mT provided by a pair of Helmholtz coils and heated to about $110 - 130\,^\circ$C. At an incident laser power of 16 W (wavelength $\lambda = 794.8$ nm), it took several minutes to achieve ^{129}Xe nuclear spin polarizations of typically 10%, verified by separate high-field (3T) NMR-measurements [10,16]. Subsequently, the spin-polarized Xe gas was expanded into always the same evacuated uncoated spherical Duran glass bulb (outer diam.: 5 cm) at room temperature. The resulting pressure inside

[a] e-mail: wolfgang.kilian@ptb.de

[b] present address: Federal Mogul Wiesbaden GmbH & Co. KG, Stielstr. 11, 65201 Wiesbaden

this glass bulb was adjusted by further expansion into additional evacuated glass bulbs (5 cm or 2 cm outer diam.) or by adding the corresponding unpolarized Xe/N_2 mixture. The exact gas pressure within the dedicated glass bulb was deduced directly after each SQUID measurement by expanding the gas into a calibrated vacuum system with a pressure gauge.

The free precession of the ^{129}Xe magnetization in low magnetic fields was recorded inside a magnetically shielded room (BMSR [17], 2.2 m×2.2 m×2.3 m, shielding factor ≥ 10000), using a vertical (z_L-direction) one-channel low-T_C DC SQUID gradiometer with a white noise level of $\sqrt{S_B} = 4.5\,\mathrm{fT}/\sqrt{\mathrm{Hz}}$ (sampling rate 50 Hz), given by the square root of the noise power spectral density S_B [18].

When entering the BMSR, the strength of the ambient magnetic field drops within 0.5 m from about 50 μT (earth's field) to tens of nT. On entering the BMSR, the bulb was carried at a velocity of > 1 m/s, which turned out to be sufficiently fast for the ^{129}Xe nuclear magnetization to maintain its initial orientation in space and not to follow the changing direction of the local ambient field adiabatically. In this way the free precession of the nuclear magnetization around the ambient magnetic field inside the BMSR was initiated. The bulb was placed directly beneath the liquid helium dewar which contained the SQUID detectors. Inside the BMSR, the residual magnetic field was about 5 nT and oriented almost vertically, known from measurements using a three-axes fluxgate (Bartington, Oxford, GB). Residual magnetization present in the μ-metal sheets of the walls of the BMSR after demagnetization contributes significantly to the residual magnetic field inside the BMSR and, therefore, its variation along various directions, e.g. along the $\boldsymbol{x}_\mathrm{L}$-, $\boldsymbol{y}_\mathrm{L}$- and $\boldsymbol{z}_\mathrm{L}$-axes of the laboratory coordinate system, are generally different. A pair of Helmholtz coils (diameter: 1 m) allowed the application of additional magnetic fields of some tens of nT along the $\boldsymbol{y}_\mathrm{L}$-direction of the laboratory coordinate system, the origin of which was taken in the following to be at the center of the glass bulb (s. Fig. 1).

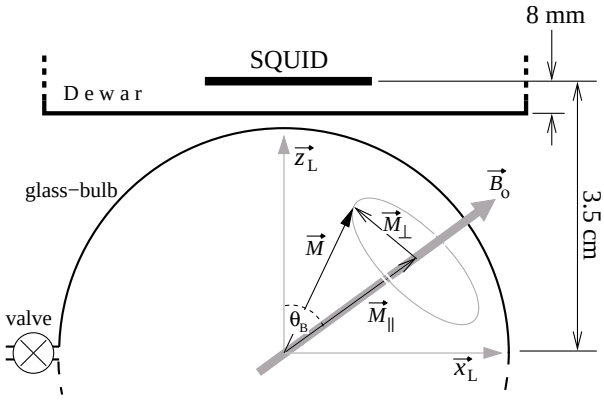

Fig. 1. Schematics of the experimental arrangement inside the BMSR, illustrating the precession of the ^{129}Xe magnetization $\boldsymbol{M}$ with components parallel ($\boldsymbol{M}_\parallel$) and perpendicular ($\boldsymbol{M}_\perp$) to the ambient magnetic field $\boldsymbol{B_0}$, tilted by θ_B from the vertical direction ($\boldsymbol{z}_\mathrm{L}$); the angle θ_B is exaggerated for clarity; the horizontal axes $\boldsymbol{x}_\mathrm{L}$, $\boldsymbol{y}_\mathrm{L}$ of the laboratory coordinate system were oriented perpendicularly to the walls of the BMSR; the distance between the plane of the lowest SQUID detector of the gradiometer and the outer surface of the bottom of the Dewar ('cold-warm distance') was 8 mm, the sample-detector distance amounted to 3.5 cm.

3 Results

In Fig. 2 we show the output signal of the one-channel SQUID gradiometer versus the observation time t, induced by the oscillating vertical component $\tilde{B}_{z_L}$ of the magnetic field produced by the precessing ^{129}Xe magnetization. The data were recorded at a total pressure of $p = (162 \pm 9)$ mbar ((130 ± 7) mbar Xe, (32 ± 2) mbar N_2) without an additional external magnetic field applied. The raw data were high-pass filtered (cut-off frequency $f_{co} = 0.02$ Hz) in order to remove any drifts and electronic offset, and fitted to the expression $\tilde{B}_{z_L}(t) = A\,\exp(-t/T_2)\,\sin(\omega t + \phi)$ to deduce the Larmor frequency $\omega = \gamma B_0$ and the transverse relaxation time T_2. Initial estimates for both parameters were deduced from Fourier-transformed high-pass filtered data. The component $\boldsymbol{M}_\perp$ of the nuclear magnetization $\boldsymbol{M}$ perpendicular to and precessing around the ambient magnetic field $\boldsymbol{B_0} = 1/V \int \boldsymbol{B}(\boldsymbol{r})dV$, averaged over the volume V of the glass bulb, caused the observed variation of the output voltage. From the data shown in Fig. 2 we deduced $\nu = \omega/2\pi = (55.340 \pm 0.001)$ mHz and $T_2 = (2330 \pm 10)$ s, which corresponds to a Larmor precession period of (18.070 ± 0.003) s and an average ambient magnetic field strength $B_0 = (4.6660 \pm 0.0001)$ nT. No drift in the Larmor precession frequency ω during the measurement time was revealed by the fit of the expression for $\tilde{B}_{z_L}$ to the measured data (s. Fig. 2) despite their high signal to noise ratio of typically 400:1 (≈ 10 pT signal amplitude and ≈ 25 fT noise level using 25 Hz bandwidth). A longitudinal relaxation of the magnetization, resulting in slow drifts of the SQUID signal integrated over the precession period, could not be measured in this way. Assuming a ^{129}Xe polarization of 0.1, a distance of 3.5 cm between the SQUID detector and the center of the spherical bulb (s. Fig. 1) filled with 200 mbar of Xe (natural abundance), $\boldsymbol{M}$ to be oriented vertically, and $\boldsymbol{B_0}$ pointing along the x_L-axis, the maximum dipolar field attainable at the detector is calculated to be about 150 pT. The smaller field amplitudes observed (≤ 20 pT) are explained by an angle of less than 90° between $\boldsymbol{B_0}$ and $\boldsymbol{M}$, and by $\boldsymbol{B_0}$ not being oriented horizontally. Also, a somewhat lower polarization due to the longitudinal relaxation during transport of the glass bulb from the laser laboratory to the magnetically shielded room may explain the lower signals observed. Since we used a spherical glass bulb, the demagnetization field $\boldsymbol{B_{de}} = -\mu_0 \boldsymbol{M}/3$ did not exert a torque on the nuclear magnetization itself and hence did not contribute to the Larmor precession frequency.

We recorded the free spin precession of ^{129}Xe at total pressures ranging from 30 mbar up to 850 mbar at two average field strengths, $B_0 \approx 4.5$ nT (ambient magnetic field) and $B_0 \approx 15$ nT, applying an additional horizontally orientated magnetic field by means of the Helmholtz coils.

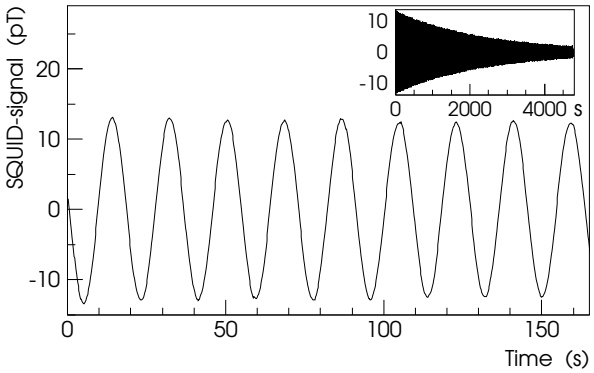

Fig. 2. Free precession of the ^{129}Xe magnetization (gas pressure $p = (162 \pm 9)$ mbar) measured with the SQUID-gradiometer. The insert shows the signal observed over an extended period of time. From the fitting procedure (see text) one obtains for the prcession frequency $\nu = (55.340 \pm 0.001)$ mHz ($\rightarrow B_0 = (4.6660 \pm 0.0001)$ nT) and a transverse relaxation time of $T_2 = (2330 \pm 10)$ s.

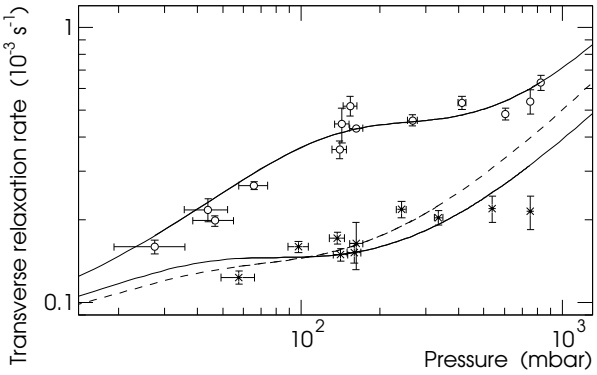

Fig. 3. Pressure dependence of the transverse relaxation rate ($1/T_2$) of Xe/N_2 gas mixtures ($p_{Xe} : p_{N_2} \approx 4 : 1$) at $B_0 \approx 4.5$ nT ($\circ$) and $B_0 \approx 15$ nT ($\times$) and fits (solid lines) of Eq. (1) to experimental data. The dashed line represents the fit ($B_0 \approx 15$ nT) omitting the data points exceeding 400 mbar (see text). Eq. (1) was augmented by the constant background rate $1/T_{2b} = 0.07 \times 10^{-3}\,\mathrm{s}^{-1}$.

For each measurement the data acqusition times were in the range of half an hour to one hour, typically, depending on the signal lifetime. Fig. 3 displays the pressure dependence of the transverse relaxation rate $1/T_2$. As can be seen, at the lower field strength, $1/T_2$ initially increases linearly with pressure and then levels off at pressures exceeding 200 mbar. Generally, lower relaxation rates were measured with the additional magnetic field applied, and relaxation times T_2 up to (8100 ± 400) s ($p = (60 \pm 9)$ mbar) were observed.

In the following, we show that the observed relaxation can be understood as due to restricted diffusion of xenon atoms in the presence of ambient static magnetic field gradients. In order to estimate such gradients, we simultaneously recorded the spin precession originating from two adjacent glass bulbs, each containing the same hyperpolarized gas mixture. The bulbs were placed beneath the dewar, with their centers 8 cm apart from each other and their symmetry axis pointing along either the (horizontal) $\boldsymbol{x}_\mathrm{L}$- or the $\boldsymbol{y}_\mathrm{L}$-axis. Fig. 4 shows the beating pattern obtained along the $\boldsymbol{y}_\mathrm{L}$-axis with no additional magnetic field applied. From the difference $\Delta\nu = (0.011 \pm 0.001)$ Hz between the Larmor frequencies, an ambient magnetic field gradient of $\Delta B_0/8$ cm $= (0.12 \pm 0.01)$ nT/cm is deduced. Generally, the magnetic field gradients along the $\boldsymbol{x}_\mathrm{L}$- and $\boldsymbol{y}_\mathrm{L}$-axis ranged between 0.01 nT/cm and 0.2 nT/cm with or without additional magnetic field applied. Similar variations of the residual magnetic field inside the BMSR have previously been deduced from fluxgate measurements [17]. As discussed above, residual magnetic field gradients are generally different along the $\boldsymbol{x}_\mathrm{L}$- and $\boldsymbol{y}_\mathrm{L}$-axes despite the quadratic cross section of the BMSR because of contributions from the residual magnetic flux in the μ-metal sheets of the walls after demagnetization. In contrast, a dipole-dipole interaction between the ^{129}Xe magnetizations in both glass bulbs cannot explain the magnitude of the difference between the Larmor frequencies. Assuming, as above, $P_{Xe} = 0.1$, $p_{Xe} = 200$ mbar and a distance of 8 cm between the centers of the spheres, the maximum dipolar interaction can be estimated to be $\Delta\nu_\mathrm{dipole} = 0.08$ mHz, about one to two orders of magnitude smaller than the observed beating. Such a small difference in the precession frequencies would not have been resolved in our measurements.

4 Comparison to theory

A theoretical treatment of the nuclear spin relaxation of rare gases due to magnetic field inhomogeneities at low magnetic fields and low pressures was reported by Cates et al. [11], taking restricted diffusion and the influence of the local magnetic field $\boldsymbol{B}(\boldsymbol{r}) = \boldsymbol{B_0} + \boldsymbol{B_1}(\boldsymbol{r})$ into account, but neglecting collisional relaxation within the gas and relaxation at the walls of the spherical cell of radius R. The deviation $\boldsymbol{B_1}(\boldsymbol{r})$ of the local field from the average homogeneous field $\boldsymbol{B_0}$ was approximated by the linear gradient fields $\boldsymbol{B_1}(\boldsymbol{r}) = \boldsymbol{r} \cdot \boldsymbol{\nabla B_1}$, with $\boldsymbol{\nabla B_1}$ being a traceless, symmetric second-rank tensor, taken to be independent of position. For the transverse relaxation rate, Cates et al. obtained

$$\frac{1}{T_2} = \frac{8R^4\gamma^2\left|\boldsymbol{\nabla} B_{1z}\right|^2}{175\,D} + D\,\frac{\left|\boldsymbol{\nabla} B_{1x}\right|^2 + \left|\boldsymbol{\nabla} B_{1y}\right|^2}{B_0^2} \times \sum_n \frac{1}{[x_{1n}^2 - 2]\left[1 + x_{1n}^4\,(\gamma B_0 R^2/D)^{-2}\right]}\,, \quad (1)$$

where D is the diffusion coefficient of the rare gas. In Eq. (1) the components of $\boldsymbol{B_1}$ refer to a coordinate system with its z-axis pointing along the average field $\boldsymbol{B_0}$. The first term represents the usual secular broadening and is proportional to the pressure p, since at constant temperature $pD(p) = p_0 D_0$, with D_0 being the diffusion coefficient at $p_0 = 1013$ mbar. The second term corresponds to lifetime broadening, where the sum runs over all zeros x_{1n} ($n = 1, 2, 3, \ldots$) of the derivative $(d/dx)\,j_1(x) =$

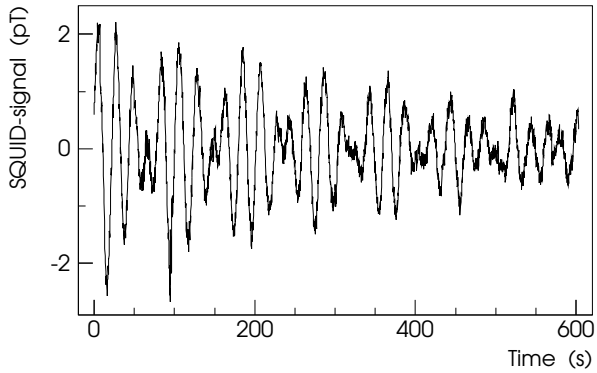

Fig. 4. Beating signals produced by the ^{129}Xe magnetization contained in two adjacent glass bulbs of the same size ($R = 2.5\,\mathrm{cm}$), separated by 8 cm and oriented along the $\boldsymbol{y}_\mathrm{L}$-axis. The different precession frequencies reflect the different ambient magnetic fields at both bulbs.

0 of the spherical Bessel function $j_1(x)$. We have verified numerically that for our experimental conditions only the first term ($x_{11} = 2.081576$) of the sum needs to be taken into account. At sufficiently low pressures, such that $\tau_D/\tau_L \ll 1$, the second term of Eq. (1) is also proportional to p, where $\tau_D = R^2/D$ is the characteristic diffusion time for a spherical cell, defined by Cates et al. [11], and $\tau_L = (\gamma B_0)^{-1}$ is $1/(2\pi)$ times the Larmor precession period. In this pressure range, motional narrowing occurs. At higher pressures at which $\tau_D/\tau_L \gg 1$, the second term of Eq. (1) decreases proportional to $1/p$. At pressures where $\tau_D/\tau_L \approx 4$ the second term in Eq. (1) gives its maximum contribution to $1/T_2$ and sets the transition between the low- and the high-pressure behavior [19]. Furthermore, the perturbation calculation leading to Eq. (1) requires $\gamma\,|\boldsymbol{B_1}|\,\tau_D \ll 1$ [11].

Cates et al. [19] measured the longitudinal relaxation rate $1/T_1$ of hyperpolarized ^{129}Xe at high pressures ($\tau_D/\tau_L \gg 1$) and the longitudinal and transverse relaxation rates $1/T_{1r}$, $1/T_{2r}$ in the rotating coordinate frame at lower pressures, i.e. for $\tau_D/\tau_R \ll 1$, where τ_R is $1/2\pi$ times the Rabi precession period. McGregor [20] investigated the gradient dependence of the T_2-relaxation of hyperpolarized ^{3}He in the high-pressure regime. To our knowledge, no direct measurements of the transverse relaxation rate $1/T_2$ of the ^{129}Xe magnetization under motional narrowing conditions, i.e. in the low-pressure regime, have been available up to now.

The experiments reported in this paper were primarily performed having future applications of spin-polarized noble gases for biomedical measurements in mind. They were not intended to determine the ambient magnetic field gradient tensor from the pressure dependence of the transverse relaxation rate. Nevertheless we have fitted (s. Fig. 3, solid lines) Eq. (1) - augmented by a background rate $1/T_{2b}$ assumed to be independent of pressure p - to our experimental data, with $|\boldsymbol{\nabla} B_{1z}|^2$ and $|\boldsymbol{\nabla} B_{1\perp}|^2 = |\boldsymbol{\nabla} B_{1x}|^2 + |\boldsymbol{\nabla} B_{1y}|^2$ being free parameters. The background relaxation rate $1/T_{2b} = 0.07 \times 10^{-3}\,\mathrm{s}^{-1}$ was obtained by extrapolating the low-field data ($p < 100\,\mathrm{mbar}$) shown in Fig. 3 to $p = 0\,\mathrm{mbar}$. The nature of the constant background relaxation rate is not precisely known, probably wall relaxation contributes to this rate. Since not enough information is available to determine wall relaxation any further, we have chosen to make the simplest assumption possible, i.e. that of a pressure independent background rate. Recently, the longitudinal relaxation rate of hyperpolarized ^{3}He in magnetized glass cells was reported to depend linearly on pressure [21,22]. However, after demagnetization of the spin exchange cells a background longitudinal relaxation rate independent of pressure was observed by Jacob et al. [22], supporting our assumption.

The self-diffusion coefficient D_0(Xe-Xe) of xenon at room temperature is about $0.06\,\mathrm{cm^2 s^{-1}}$ as measured by various methods [23–25]. The diffusion coefficient of xenon for infinite dilution of xenon in nitrogen is given as $D_0(\mathrm{Xe\text{-}N_2}) = 0.21\,\mathrm{cm^2 s^{-1}}$ [26]. Linearly interpolating the inverse of these diffusion coefficients - plotted versus the xenon mole fraction - to the gas mixture used in our experiments ($80\,vol.\%$ Xe, $20\,vol.\%$ N_2), we get $D_0(\mathrm{Xe{:}N_2} = 4:1) \approx 0.07\,\mathrm{cm^2 s^{-1}}$ at 293 K. With this input value we obtain $|\boldsymbol{\nabla} B_{1z}| = (0.07 \pm 0.002)\,\mathrm{nT/cm}$ and $|\boldsymbol{\nabla} B_{1\perp}| = (0.16 \pm 0.003)\,\mathrm{nT/cm}$ ($B_0 \approx 4.5\,\mathrm{nT}$) and $|\boldsymbol{\nabla} B_{1z}| = (0.05 \pm 0.002)\,\mathrm{nT/cm}$, $|\boldsymbol{\nabla} B_{1\perp}| = (0.14 \pm 0.007)\,\mathrm{nT/cm}$ ($B_0 \approx 15\,\mathrm{nT}$) from the fit. These values are well within the range of the gradients estimated from the spin precession of the ^{129}Xe contained in two adjacent spherical bulbs. Since the ambient magnetic field ($B_0 \approx 4.5\,\mathrm{nT}$) was essentially vertically oriented but the sum of the ambient and external magnetic field ($B_0 \approx 15\,\mathrm{nT}$) almost horizontally ($\theta_B = 70°$), different gradients $|\boldsymbol{\nabla} B_{1z}|$ and $|\boldsymbol{\nabla} B_{1\perp}|$ are to be expected at both field strengths.

For our conditions, the transition between the low- and high-pressure behavior is calculated to occur at $p \approx 150\,\mathrm{mbar}$ for the measurements at $B_0 \approx 4.5\,\mathrm{nT}$. This is reflected in our experimental data. Furthermore, at pressures $p < 100\,\mathrm{mbar}$, $1/T_2$ increases linearly with the pressure - as predicted by theory -, and motional narrowing is observed. For pressures $150\,\mathrm{mbar} \le p \le 500\,\mathrm{mbar}$, the pressure dependence of the first term ($\propto p$) and of the second term ($\propto 1/p$) of Eq. (1) compensate each other approximately.

Due to the $1/B_0^2$ dependence of the second term in Eq. (1), lower relaxation rates are recorded at the higher field strength ($B_0 \approx 15\,\mathrm{nT}$). Whilst Eq. (1) quantitatively explains our low-field data, there are some discrepancies between theory (Fig. 3 solid line) and experiment at the higher field strength. For $B_0 \approx 15\,\mathrm{nT}$, theory predicts the transition between the low- and the high-pressure behavior to take place at $p \approx 50\,\mathrm{mbar}$ just below the lowest pressure at which relaxation was measured at the higher field strength. In addition this transition is more difficult to observe since the measured relaxation rates are close the background rate $1/T_{2b}$. As mentioned above, Eq. (1) requires $\gamma\,|\boldsymbol{B_1}|\,\tau_D \ll 1$. Taking $|\boldsymbol{\nabla} \boldsymbol{B_{1\perp}}| \approx 0.15\,\mathrm{nT/cm}$, we estimate the pressure at which $\gamma R\,|\boldsymbol{\nabla} \boldsymbol{B_{1\perp}}|\,\tau_D \approx 1$ to be $p \approx 460\,\mathrm{mbar}$. Hence, for pressures exceeding 400 mbar, Eq. (1) might not be strictly valid. The two data points shown in Fig. 3 taken

at $B_0 \approx 15\,\mathrm{nT}$ and exceeding this pressure might indicate the breakdown of first order perturbation theory or represent outliers. On the other hand, at the lower field strength ($B_0 \approx 4.5\,\mathrm{nT}$) no discrepancies are observed in this pressure range (s. Fig. 3). Restricting the high-field fit to data points measured below $p = 400\,\mathrm{mbar}$ we obtain a considerably improved description of the measured relaxation rates (Fig. 3 dashed line), yet with resulting field gradients ($|\boldsymbol{\nabla} B_{1z}| = (0.06 \pm 0.002)\,\mathrm{nT/cm}$, $|\boldsymbol{\nabla} B_{1\perp}| = (0.12 \pm 0.01)\,\mathrm{nT/cm}$) being very similar to the ones mentioned above.

Furthermore, the relaxation due to the secular contribution to $1/T_2$ (first term in Eq. (1)), which is proportional to pressure p, cannot rise ad infinitum. At some point diffusion will be so slow that it no longer will contribute to relaxation. From that point on any further increase of pressure will no longer change the relaxation rate. Without relying on first-order perturbation theory, the pressure range at which the secular contribution begins to saturate was estimated from Monte Carlo (MC) calculations. Numerical simulations were carried out for various pressures up to 10 bar, taking the experimental conditions into account and neglecting lifetime broadening as well as collisional and wall relaxation. To this end we followed the diffusion of a nuclear spin-polarized ^{129}Xe atom placed at random within the glass cell at $\boldsymbol{r_0} = \boldsymbol{r}(t = 0)$, and, every $\Delta t = 10\,\mathrm{ms}$, sampled the change $\Delta\varphi = \gamma \Delta t (B_0 + \boldsymbol{\nabla} B_{1z} \Delta \boldsymbol{r})$ in phase angle φ of its magnetic moment perpendicular to the homogeneous average field $\boldsymbol{B_0}$ ($B_0 = 15\,\mathrm{nT}$), as the atom moves from position $\boldsymbol{r}(t)$ to position $\boldsymbol{r}(t + \Delta t) = \boldsymbol{r} + \Delta \boldsymbol{r}$. The time increment $\Delta t = 10\,\mathrm{ms}$ was chosen sufficiently small to result in small phase changes, e.g. at $B_0 = 15\,\mathrm{nT}$, $|\boldsymbol{\nabla} B_{1z}| = 0.15\,\mathrm{nT/cm}$ and $\Delta z = \sqrt{2D\Delta t} = 0.119\,\mathrm{cm}$ ($p = 100\,\mathrm{mbar}, T = 293\,\mathrm{K}$), $\Delta\varphi = 0.011\,\mathrm{rad}$. It should be noted that the time increment Δt is considerably longer than the gas collision time $\tau_c \approx 3.7\,\mathrm{ns}$ at 100 mbar. Depending on pressure and the value chosen for $|\boldsymbol{\nabla} B_{1z}|$, taken to be independent of position, the diffusion of the atom was followed for times t up to 1000 s, i.e. for $N = 10^5$ steps. This process was repeated for a total of 2000 spin-polarized ^{129}Xe atoms all starting with the same perpendicular component of their magnetic moment taken parallel to the surface normal of the detector. Subsequently for each observation time $t = N\,\Delta t$ the total magnetization along the surface normal was calculated, resulting in a free induction decay, from which the secular contribution to the transverse relaxation was inferred (see Fig. 5).

At pressures $p < 3\,\mathrm{bar}$, the results of our MC calculations agree well with the first term of Eq. (1) for the gradients $|\boldsymbol{\nabla} B_{1z}|$ up to $0.15\,\mathrm{nT/cm}$ (s. Fig. 5). A saturation of the secular contribution to $1/T_2$ was observed for pressures exceeding 3 bar, approximately. This implies that the levelling off observed in Fig. 3 cannot be explained solely by the secular term, i.e. by restricted diffusion in the presence of a field gradient $\boldsymbol{\nabla} B_{1z}$, but that it reflects the interplay of both terms of Eq. (1).

The collisional relaxation caused by the spin-rotation interaction $\gamma \boldsymbol{N} \boldsymbol{I}$ between the ^{129}Xe nuclear spin $\boldsymbol{I}$ and the molecular angular momentum $\boldsymbol{N}$ during ^{129}Xe-Xe collisions is important at high pressures, limiting the longitudinal relaxation time to $T_1 = 56/(\rho/\rho_{\mathrm{ST}})\,\mathrm{h}$ [27], where ρ/ρ_{ST} is the atomic density normalized to its value at $T_0 = 273.15\,\mathrm{K}$ and $p_0 = 1013\,\mathrm{mbar}$. In our case, however, contributions of the collisional relaxation to the transverse relaxation rate can be neglected due to the low atomic densities ($\rho \leq 0.78/\rho_{\mathrm{ST}}$) used.

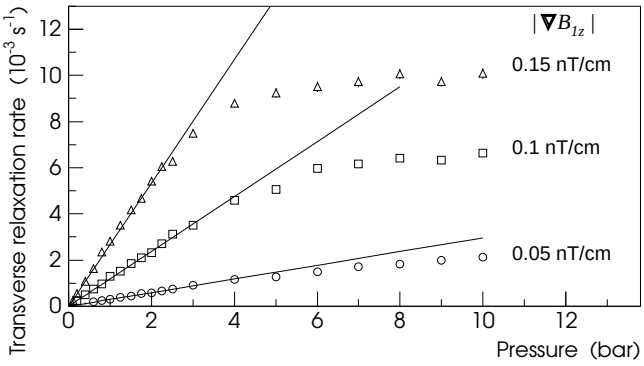

Fig. 5. Secular contribution to the transverse relaxation rate, calculated for three different gradients $|\boldsymbol{\nabla} B_{1z}|$ by Monte Carlo simulations (symbols) and by the first term of Eq. (1) (solid lines) assuming $B_0 = 15\,\mathrm{nT}$.

5 Conclusion

The transverse relaxation of hyperpolarized ^{129}Xe produced off-line, was studied quantitatively at room temperature in ultra-low external magnetic fields ($B_0 = 4.5 - 15\,\mathrm{nT}$). The observed pressure dependence of the transverse relaxation rate confirmed the predictions of an existing theory of spin relaxation in the motional narrowing regime.

The high signal-to-noise ratio in the detection of the oscillating magnetic field produced by the precessing ^{129}Xe magnetization and the long transverse relaxation times T_2 observed (up to 8000 s) support the idea that hyperpolarized rare gases can indeed be used for several new applications, e.g. for SQUID-NMR, as a tool for nuclear thermometry, or as a highly sensitive absolute magnetometer (reviewed in [28]). By employing hyperpolarized ^{3}He with a self-diffusion coefficient which is more than one order of magnitude larger than that of xenon ($D_0(\mathrm{He}) \approx 2\,\mathrm{cm}^2/\mathrm{s}$ [29]) at pressures as low as one mbar, and by using glass containers with a very low wall relaxation [21], transverse relaxation times in the range of one day and longer should be attainable.

Furthermore, by using multi-channel SQUID-detectors [30] it may also be possible to perform spatially resolved measurements without having to use switched magnetic field gradients as in MRI measurements. This may open the way to using hyperpolarized rare gases as agents for spatially resolved biomagnetic measurements [31].

We acknowledge the help of A. Schnabel and W. Müller during measurements. Also, we would like to thank L.

Trahms, B Ittermann and L. Mitschang for fruitful discussions.

References

1. T. Walker, W. Happer, Rev. Mod. Phys. **69**, 629 (1997)
2. I.C. Ruset, S. Ketel, F.W. Hersman, Phys. Rev. Lett. **96**(053002), 1 (2006)
3. R. Surkau, J. Becker, M. Ebert, T. Grossmann, W. Heil, D. Hofmann, H. Humbolt, M. Leduc, E. Otten, D. Rohe et al., Nucl. Inst. and Meth. **A 384**, 444 (1997)
4. P.L. Anthony, et al., Phys. Rev. Lett. **71**, 959 (1993)
5. D. Bear, T.E. Chupp, K. Cooper, S. DeDeo, M. Rosenberry, R.E. Stoner, R.L. Walsworth, Phys. Rev. A **57**, 5006 (1998)
6. D. Bear, R.E. Stoner, R.L. Walsworth, Phys. Rev. Lett. **85**, 5038 (2000), Erratum: Phys. Rev. Lett. 89, 209902(E) (2002)
7. M.S. Albert, G.C. Cates, B. Driehuys, W. Happer, B. Saam, C.S. Springer Jr, A. Wishnia, Nature **370**, 199 (1994)
8. M. Ebert, T. Grossmann, W. Heil, W.E. Otten, R. Surkau, M. Leduc, P. Bachert, M.V. Knopp, L.R. Schad, M. Thelen, Lancet **347**, 1297 (1996)
9. S.D. Swanson, M.S. Rosen, B.W. Agranoff, K.P. Coulter, R.C. Welsh, T.E. Chupp, Magn. Reson. Med. **38**, 695 (1997)
10. W. Kilian, F. Seifert, H. Rinneberg, Magn. Reson. Med. **51**, 843 (2004)
11. G.D. Cates, S.R. Shaefer, W. Happer, Phys. Rev. A **37**, 2877 (1988)
12. C. Cohen-Tannoudji, DuPont-Roc, Haroche, Laloe, Phys. Rev. Lett. **22**, 758 (1969)
13. S.A. Gudoshnikoov, A.N. Kozlov, Y.V. Maslennikov, A.Y. Serebrjakov, O.V. Snigirev, IEEE **27**, 2449 (1991)
14. D.M. TonThat, M. Ziegeweid, Y.Q. Song, E.J. Munson, S. Appelt, A. Pines, J. Clarke, Chem. Phys. Lett. **272**, 245 (1997)
15. M.P. Augustine, A. Wong-Foy, J.L. Yarger, M. Tomaselli, A. Pines, D.H. TonThat, J. Clarce, Appl. Phys. Lett. **72**, 1908 (1998)
16. W. Kilian, Ph.D. thesis, Freie Universität Berlin (2001), www.diss.fu-berlin.de/2001/105/
17. S.N. Erné, H.D. Hahlbohm, H. Scheer, Z. Trontlelj, *The Berlin Magnetically Shielded Room - Performances*, in *Biomagnetism*, edited by S.N. Erné, H.D. Hahlbohm, H. Lübbig (Walter de Gruyter, Berlin, New York, 1981), pp. 79–87
18. H. Matz, D. Drung, S. Hartwig, H. Gross, R. Kötitz, W. Müller, A. Vass, W. Weitschies, L. Trahms, Appl. Superconductivity **6**, 577 (1999)
19. G.D. Cates, D.J. White, T.C. Chien, S.R. Schaefer, W. Happer, Phys. Rev. A **38**, 5092 (1988)
20. D.D. McGregor, Phys. Rev. A **41**(5), 2631 (1990)
21. J. Schmiedeskamp, H.J. Elmers, W. Heil, E.W. Otten, Y. Sobolev, W. Kilian, H. Rinneberg, T. Sander-Thoemmes, F. Seifert, J. Zimmer, Eur. Phys. J. D **38**, 445 (2006)
22. R.E. Jacob, S.W. Morgan, B. Saam, J.C. Leawoods, Phys. Rev. Lett. **87**, 143004,1 (2001)
23. J.O. Hirschfelder, C.F. Curtis, R.B. Brid, *Molecular Theory of Gases and Liquides* (Wiley, New York, 1954), p. 581
24. H. Watts, Can. J. Chem. **43**, 431 (1965)
25. R.W. Mair, D.G. Cory, S. Peled, C.H. Tseng, S. Patz, R.L. Walsworth, J. Mag. Res. **135**, 478 (1998)
26. K.C. Hasson, G.D. Cates, K. Lerman, P. Bogorad, W. Happer, Phys. Rev. A **41**, 3672 (1990)
27. E.R. Hunt, H.Y. Carr, Phys. Rev. **130**, 2302 (1963)
28. Y.S. Greenberg, Rev. Mod. Phys. **70**, 175 (1998)
29. X.J. Chen, H.E. Moeller, M.S. Chawla, G.P. Cofer, B. Driehuys, L.W. Hedlund, G.A. Johnson, Magn. Reson. Imag. **42**, 721 (1999)
30. M. Burghoff, A. Schnabel, D. Drung, F. Thiel, S. Knappe-Gruneberg, S. Hartwig, L. Kosch, O. Trahms, H. Koch, Neurol. Clin. Neurophysiol. **67**, 1 (2004)
31. F. Seifert, G. Wübbler, W. Kilian (2004), talk at the Second International Workshop on Parallel MRI, Zürich, Switzerland, http://www.mr.ethz.ch/parallelmri04/program.html